

## Calculated optical properties of zincblende semiconductors ZnTe, CdTe and HgTe

This article has been downloaded from IOPscience. Please scroll down to see the full text article.

1992 J. Phys.: Condens. Matter 4 2505

(<http://iopscience.iop.org/0953-8984/4/10/014>)

View [the table of contents for this issue](#), or go to the [journal homepage](#) for more

Download details:

IP Address: 171.66.16.159

The article was downloaded on 12/05/2010 at 11:28

Please note that [terms and conditions apply](#).

## Calculated optical properties of zincblende semiconductors ZnTe, CdTe and HgTe

Roman Markowski and Marek Podgórný

Instytut Fizyki, Uniwersytet Jagielloński, 30-059 Kraków, ul Reymonta 4, Poland

Received 15 March 1991, in final form 25 October 1991

**Abstract.** Self-consistent semi-relativistic linear muffin-tin orbital calculations of the band structures are used in conjunction with the local-density approximation to derive the complex dielectric function,  $\epsilon(\omega) = \epsilon_1(\omega) + i\epsilon_2(\omega)$ , and the reflectivity spectrum  $R(\omega)$  up to 20 eV for the three most common II–VI semiconducting compounds ZnTe, CdTe and HgTe. We have interpreted the sharp structures above approximately 9 eV as transitions originating in the metal d levels. It is shown that a very significant contribution to the reflectivity spectrum in the UV energy range arises from the transitions originating in the upper part of the valence band to the higher conduction bands.

### 1. Introduction

In the last 20 years the electronic properties of the zincblende semiconductors ZnTe, CdTe and HgTe have been studied extensively both experimentally and theoretically. Band structure calculations have been carried out using different approaches [1–7] and probed by means of several experimental techniques: reflectivity [8], modulation spectroscopy [9], ultraviolet [10] and x-ray photoemission [11].

The aim of this work is to derive the real and imaginary parts of the dielectric function as well as the reflectivity spectrum in the semiconducting compounds ZnTe, CdTe and HgTe. These three most common II–VI semiconductors are characterized by wide, medium and narrow forbidden energy gaps (2.25 eV, 1.59 eV and –0.31 eV respectively at room temperature). The imaginary part of the dielectric function is calculated both in a constant matrix element approximation and with  $k$ -dependent matrix elements. The theoretical results obtained in the present calculations are compared with experimental measurements performed by Kisiel *et al* [8] and Cardona and Greenaway [12] in order to verify the interpretation of reflectivity spectra for these materials. The calculations not only support the common belief that the structures in the energy region above 9 eV can be attributed to transitions beginning in the uppermost d levels of the cation but also reveal a very significant contribution to the reflectivity spectrum which arises from transitions to the higher conduction bands. Furthermore, we discuss the core exciton interpretation for some structures in the reflectivity spectra.

In general, good qualitative agreement with experiment is obtained [8] although, as usually observed in the LDA calculations, all peaks are located at too low an energy.

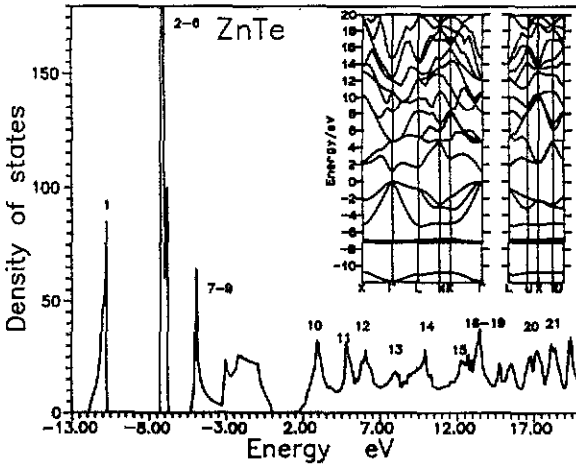


Figure 1. Total density of states for ZnTe. Figures near the main peaks on the curve denote the serial numbers of the bands. The calculated band structure is shown in the inset.

The presentation is organized as follows: the outline of the theoretical calculations is presented in section 2. The results and the discussion are presented in section 3. A brief summary is given in section 4.

## 2. Method of calculation

The LMTO method which we used in this study of the optical properties of ZnTe, CdTe and HgTe is described elsewhere [13] and the details of its application to the calculation of the electronic structure of the zincblende-type compounds are presented in another paper [14]. The band structures were calculated with the inclusion of the 'combined correction term' [13]. Scalar relativistic corrections, very important in the case of this study, were also consistently applied (i.e. all relativistic effects except the spin-orbit coupling were included). The exchange-correlation LDA potential was used in the form proposed by Vosko, Wilk and Nusair [15].

The crystal structures were considered as FCC lattices with four sites on the basis, Cd, Te, E1 and E2 (taking CdTe as an example), where E1 and E2 denote the positions at which the 'empty spheres' are centred ( $Z = 0$ ) [16, 17]. In the zincblende structure the spheres are located at the following positions of the unit cell: cation (0, 0, 0), Te(1/4, 1/4, 1/4), E1(1/2, 1/2, 1/2) and E2(3/4, 3/4, 3/4). Experimental lattice constants (6.086 Å, 6.462 Å and 6.456 Å for ZnTe, CdTe and HgTe respectively) were used throughout the calculations and the ratios of atomic sphere radii for the cation, Te, and the empty spheres were set at 1.25:1.25:1 for CdTe and HgTe and at 1.1:1.25:1 for ZnTe. 240  $k$  points were used during the self-consistency procedure. All calculations were carried out in a single energy panel using 5s, 5p and 5d based functions for Te and ns, np, and  $(n-1)d$  functions with  $n = 4, 5$  and 6 for Zn, Cd and Hg respectively.

The optical absorption is proportional to the imaginary part of the dielectric function  $\epsilon(\omega, q)$  with  $q \cong 0$  in the optical range. In the limit of vanishing linewidth, the imaginary part of the dielectric function is given by [14, 18]:

$$\epsilon_2(\omega) \sim \omega^{-2} \sum_n \sum_m \int d^3 k |\langle nk | P | mk \rangle|^2 \delta(E_n^k - E_m^k - \hbar\omega) \quad (1)$$

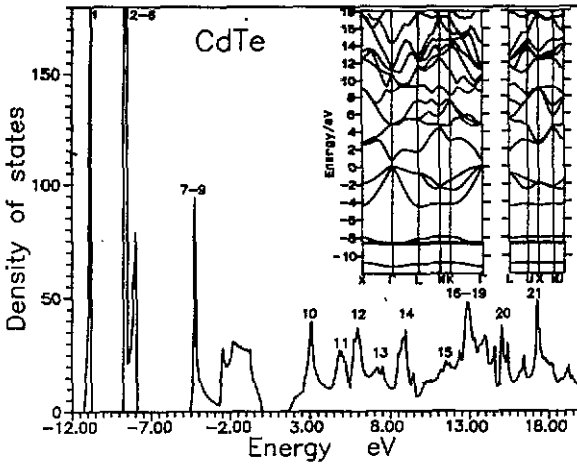


Figure 2. Total density of states for CdTe. Figures near the main peaks on the curve denote the serial numbers of the bands. The calculated band structure is shown in the inset.

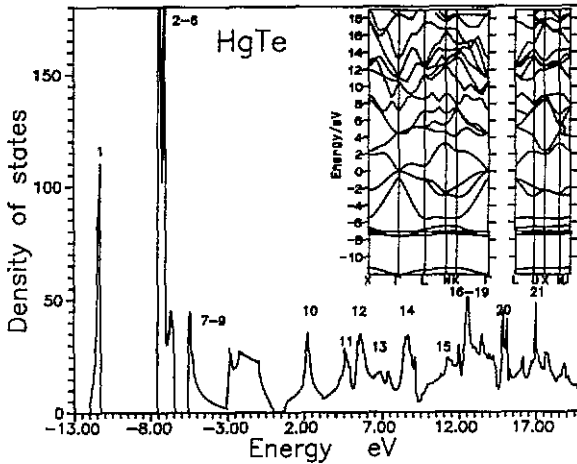


Figure 3. Total density of states for HgTe. Figures near the main peaks on the curve denote the serial numbers of the bands. The calculated band structure is shown in the inset.

where  $M_{nm}^k = \langle nk|P|mk \rangle$  is the dipole matrix element calculated with the wave function  $|nk\rangle$  expressed in terms of the one-centre expansion [13, 14]. In the present study we have fully implemented the computational scheme devised by Koenig and Khan [19] and by Alouani *et al* [20].

The imaginary part of the dielectric function,  $\epsilon_2(\omega)$ , was calculated for photon energies ranging up to 20 eV. The real part  $\epsilon_1(\omega)$  was obtained by the Kramers–Kronig transformation of  $\epsilon_2(\omega)$  in which a tail of the form  $(\beta\omega)/(\omega^2 + \gamma^2)^2$ , as described by Petroff *et al* [21], was attached for energies greater than 20 eV ( $\gamma$  is equal to 4.5 eV and  $\beta$  is determined by the continuity of  $\epsilon_2(\omega)$  at 20 eV). The reflectivity spectrum,  $R(\omega)$ , was obtained directly [2, 22] from  $\epsilon_2(\omega)$  and  $\epsilon_1(\omega)$  using the formulae:

$$\epsilon_1 = n^2 - k^2 \quad \epsilon_2 = 2nk \quad R = [(n - 1)^2 + k^2]/[(n + 1)^2 + k^2]. \quad (2)$$

The procedure for aligning the experimental and theoretical energy scales used in this study has been described in [14] and is summarized briefly in the next section.

**Table 1.** Energy values (in eV) at some high-symmetry points of the Brillouin zone from band structure calculations (this work) compared to other theoretical and experimental determinations for ZnTe.

|                 |                | Calculated<br>(without s-o) | Experiment <sup>(a)</sup> | Theory <sup>(b)</sup> |
|-----------------|----------------|-----------------------------|---------------------------|-----------------------|
| $\Gamma_{6c}$   | $\Gamma_{1c}$  | 0.00                        | 0.00                      | 0.00                  |
| $L_{6c}^1$      | $L_{1c}$       | 0.58                        | 0.73                      | 0.72                  |
| $X_{6c}$        | $X_{3c}$       | 1.07                        | 1.0                       | 1.0                   |
| DOS peak        |                | 1.26                        | 1.55                      | 1.8                   |
| $\Gamma_{7c}$   | $\Gamma_{15c}$ | 3.59                        | 3.2                       | 3.53                  |
| $\Gamma_{8c}$   |                | —                           | —                         | 3.70                  |
| $L_{6c}^2$      | $L_{3c}$       | 4.14                        | 4.35                      | 4.16                  |
| $X_{7c}$        | $X_{1c}$       | 1.24                        | —                         | 1.50                  |
| fundamental gap |                | 1.21                        | 2.25                      | —                     |
| Zn 3d threshold |                | 8.4                         | 11.75 ± 0.1 <sup>c</sup>  | —                     |
| Te 5s threshold |                | 11.85                       | 13.05 <sup>d</sup>        | —                     |

<sup>(a)</sup> From table 2 of [8].

<sup>(b)</sup> From figure 5 of [3].

<sup>(c)</sup> See [24].

<sup>(d)</sup> See [27].

### 3. Results and discussion

The highest-lying occupied d states of the cation (Zn 3d, Cd 4d, Hg 5d) in II-VI semiconducting compounds play a very important role in determining the electronic structure and optical properties of these materials [23]. The d states are situated so high in energy that they affect the fundamental gap due to hybridization to the p states at the top of the valence band. The p-d mixing is allowed by symmetry in tetrahedral compounds ( $T_{2d}$ ). In all the compounds considered the cation d bands are located above the Te 5s band.

The calculated LDA energy bands and densities of states for ZnTe, CdTe and HgTe are shown in figures 1, 2 and 3. In tables 1, 2 and 3 we summarize the eigenvalues of several conduction band states at some of the high-symmetry points. All energies (in eV) are referred to the bottom of the conduction band. The band structures agree with experiment in predicting ZnTe and CdTe to be direct-gap semiconductors, although the gaps are far too small. HgTe is a zero gap semimetal with an inverted band at the  $\Gamma$  point showing  $\Gamma_{1c}$  below  $\Gamma_{15v}$ . The binding energies of the metal d levels with respect to the top of the valence bands are too small and in disagreement with the experimental value (cation d band binding energies with respect to the valence band maximum are 9.5 eV, 10.09 eV and 7.70 eV for Zn 3d, Cd 4d and Hg 5d respectively [24]).

We have recently carried out a self-consistent band structure calculation for CdTe with a hole in the Cd 4d bands. We obtained much better agreement of the binding energy of the metal 4d levels and improved comparison with the experimental value.

When matrix elements are assumed to be constant, the resulting  $\epsilon_2(\omega)$  spectrum is proportional to the unbroadened joint density of states in which the selection rules are completely ignored. As we pointed out before [14], the constant matrix element approximation works reasonably well in the visible and near-UV range but it fails utterly

**Table 2.** Energy values (in eV) at some high-symmetry points of the Brillouin zone from band structure calculations (this work) compared to other theoretical and experimental determinations for CdTe.

|                 |                | Calculated<br>(without s-o) | Experiment <sup>(a)</sup> | Theory <sup>(b)</sup> |
|-----------------|----------------|-----------------------------|---------------------------|-----------------------|
| $\Gamma_{6c}$   | $\Gamma_{1c}$  | 0.00                        | 0.00                      | 0.00                  |
| $L_{6c}^1$      | $L_{1c}$       | 1.02                        | 1.00 <sup>(c)</sup>       | 1.23                  |
| $X_{6c}$        | $X_{3c}$       | 1.84                        | 1.77                      | 1.89                  |
| DOS peak        |                | 2.37                        | 2.22                      | 2.30 <sup>(d)</sup>   |
| $\Gamma_{7c}$   | $\Gamma_{15c}$ | 4.13                        | 3.80                      | 3.77                  |
| $\Gamma_{8c}$   |                | —                           | —                         | 4.02                  |
| $L_{6c}^2$      | $L_{3c}$       | 4.73                        | 4.45 <sup>(c)</sup>       | 4.59                  |
| $L_{4,5c}$      |                | —                           | 4.82 <sup>(c)</sup>       | 4.76                  |
| $X_{7c}$        | $X_{1c}$       | 2.10                        | —                         | 2.36                  |
| fundamental gap |                | 0.69                        | 1.59                      | —                     |
| Cd 4d threshold |                | 9.20                        | 11.59 ± 0.05              | —                     |

<sup>(a)</sup> From table 2 of [8].<sup>(b)</sup> From table 2 of [8] and from table 21 of [2].<sup>(c)</sup> From table 2 of [8] and from [2, 3, 22, 28, 29].<sup>(d)</sup> From figure 2 of [30].**Table 3.** Energy values (in eV) at some high-symmetry points of the Brillouin zone from band structure calculations (this work) compared to other theoretical and experimental determinations HgTe.

|                 |                | Calculated<br>(without s-o) | Experiment <sup>(a)</sup> | Theory <sup>(b)</sup> |
|-----------------|----------------|-----------------------------|---------------------------|-----------------------|
| $\Gamma_{8v}$   | $\Gamma_{15}$  | 0.00                        | 0.00                      | 0.00                  |
| $L_{6c}^1$      | $L_{1c}$       | 0.63                        | 1.00 <sup>(c)</sup>       | 1.20                  |
| $X_{6c}$        | $X_{3c}$       | 1.94                        | 2.50                      | 2.30                  |
| DOS peak        |                | 2.25                        | 3.10                      | 3.20 <sup>(d)</sup>   |
| $\Gamma_{7c}$   | $\Gamma_{15c}$ | 4.50                        | 5.10                      | 4.90                  |
| $\Gamma_{8c}$   |                | —                           | 5.30 <sup>(c)</sup>       | 5.30                  |
| $L_{6c}^2$      | $L_{3c}$       | 5.23                        | 5.8                       | 6.0                   |
| $L_{4,5c}$      |                | —                           | 6.2 <sup>(c)</sup>        | 6.2                   |
| $X_{7c}$        | $X_{1c}$       | 2.34                        | 3.0 <sup>(c)</sup>        | 3.2                   |
| fundamental gap |                | -0.8                        | -0.31                     | —                     |
| Hg 3d threshold |                | 7.2                         | 7.7 ± 0.01                | —                     |

<sup>(a)</sup> From table 2 of [8].<sup>(b)</sup> From figure 1 of [4].<sup>(c)</sup> From table 2 of [8] and from [24, 31, 32, 33].<sup>(d)</sup> From figure 2 of [34].

in the high-energy part of the spectrum. A quantitative comparison with experiment in the UV range is only meaningful if the matrix elements of  $P$ , the momentum operator, are included in the calculation. The positions of the peaks in  $\epsilon_2(\omega)$  compared with the experimental data and other (adjusted) calculations are given in tables 4, 5 and 6. As

**Table 4.** Experimental and theoretical values (in eV) of energy gaps in ZnTe compared to the LDA values calculated in this work.

| Peak   | Experimental         | Other calculations   | Present calculations |          |
|--------|----------------------|----------------------|----------------------|----------|
|        |                      |                      | unadjusted           | adjusted |
| $E_0$  | 2.273 <sup>(a)</sup> | 1.012 <sup>(a)</sup> | 1.21                 | 2.05     |
|        | 2.26 <sup>(a)</sup>  | —                    | —                    | —        |
|        | 2.35 <sup>(a)</sup>  | —                    | —                    | —        |
|        | 2.25 <sup>(a)</sup>  | —                    | —                    | —        |
| $E_1$  | 3.52 <sup>(a)</sup>  | 2.132 <sup>(a)</sup> | 2.68                 | 3.52     |
| $E_2$  | 5.30 <sup>(b)</sup>  | —                    | 4.46                 | 5.30     |
| $E'_1$ | 6.85 <sup>(b)</sup>  | —                    | 6.0                  | 6.84     |
| a      | 11.68 <sup>(b)</sup> | —                    | 10.81                | 11.65    |
| b      | 12.30 <sup>(b)</sup> | —                    | 11.50                | 12.34    |
| c      | 12.72 <sup>(b)</sup> | —                    | 12.02                | 12.84    |
| d      | 13.10 <sup>(b)</sup> | —                    | 10.12                | 13.17    |
| e      | 14.98 <sup>(b)</sup> | —                    | 12.04                | 15.09    |
| f      | 16.1 <sup>(b)</sup>  | —                    | 13.18                | 16.05    |
| g      | —                    | —                    | 15.84                | 16.68    |
| h      | 18.5 <sup>(b)</sup>  | —                    | 15.14                | 18.20    |

<sup>(a)</sup> See table 2 in [7];  $T = 300$  K.

<sup>(b)</sup> From table 1 of [8];  $T = 300$  K.

the LDA fails in predicting correct values for the energy gaps of semiconductors, a very simple procedure of energy band shifting has been applied which aligns the experimental and theoretical energy scales [14]. The experimental value of binding energy of metal d states was introduced into the LMTO procedure by changing the potential parameters and the full calculation of band structure was repeated. Furthermore, the conduction bands were shifted towards higher energies bringing into fair agreement the experimental and calculated positions of the  $E_0$ ,  $E_1$  and  $E_2$  maxima in the reflectivity spectra. The results of the alignment procedure are presented in figures 4, 5 and 6 as well as in tables 4, 5 and 6.

At higher energies, a wealth of sharp features appear in the absorption spectra. In our work we have studied the origins of the structures labelled in these figures: a, c, d, f, g and h situated in the energy region between 9 and 20 eV. In this region two broad reflectivity structures were found by Cardona and Greenaway [12] and attributed to the excitation of the d states. On account of the nature of the Kramers-Kronig transformation and the non-linear character of formulae connecting  $\epsilon_1(\omega)$ ,  $\epsilon_2(\omega)$  and  $R(\omega)$ , we cannot use reflectivity spectra to discuss contributions which arise from the transitions originating in the different valence bands. This is the main reason why we use  $\epsilon_2(\omega)$  spectra instead of  $R(\omega)$  in the following analysis.

The adjusted spectra of  $\epsilon_2(\omega)$  on an expanded scale (in the region of the d excitations) are presented in figures 4, 5 and 6 for ZnTe, CdTe and HgTe respectively. The short-dashed curve represents the contribution to the imaginary part  $\epsilon_2(\omega)$  which derives from transitions from the 1st band (Te 5s) to the bands lying above the Fermi level. The medium-dashed curve represents the contribution of transitions originating from the metal d levels. The long-dashed curve represents the contribution to  $\epsilon_2(\omega)$  originating from the three uppermost valence bands (namely the 7th, 8th and 9th).

**Table 5.** Experimental and theoretical values (in eV) of energy gaps in CdTe compared to the LDA values calculated in this work.

| Peak   | Experimental  | Other calculations            | Present calculations    |  |
|--------|---|-------------------------------|-------------------------|--|
|        |   |                               | unadjusted              | adjusted   |
| $E_0$  | 1.59 <sup>(a)</sup><br>1.50 <sup>(b)</sup>                        | 1.51 <sup>(g)</sup><br>—      | 0.69<br>—               | 1.56<br>—  |
| $E_1$  | 3.30 <sup>(c)</sup><br>3.44 <sup>(d)</sup><br>3.35 <sup>(b)</sup> | 3.16 <sup>(g)</sup><br>—<br>— | 2.54<br>—<br>—          | 3.37<br>—<br>—   |
| $E_2$  | 5.00 <sup>(b)</sup><br>5.40 <sup>(f)</sup>                        | 4.83 <sup>(g)</sup><br>—      | 4.50<br>4.80            | 5.20<br>5.51   |
| $E'_1$ | 6.79 <sup>(f)</sup>   | 5.76 <sup>(g)</sup>           | 5.98                    | 6.71   |
| a      | 12.17 <sup>(f)</sup>  | —                             | 11.10                   | 12.10  |
| c      | 13.36 <sup>(f)</sup>  | —                             | —                       | 13.30  |
| d      | 13.81 <sup>(f)</sup>  | —                             | 11.68                   | 13.85  |
| e      | 15.4 <sup>(f)</sup>   | —                             | 13.27                   | 15.60  |
| f      | 16.0 <sup>(f)</sup>   | —                             | 13.87                   | 16.00  |
| g      | 17.1 <sup>(f)</sup><br>—<br>—                                     | —<br>—<br>—                   | 14.32<br>14.58<br>15.64 | 16.40 <sup>(e)</sup><br>16.70 <sup>(e)</sup><br>18.00 <sup>(e)</sup> |
| h      | 19.0 <sup>(f)</sup><br>—  | —<br>—                        | 17.01<br>—              | 18.8 <sup>(e)</sup><br>19.6 <sup>(e)</sup>                           |

<sup>(a)</sup> From [35];  $T = 1.6$  K.<sup>(b)</sup> From [36];  $T = 300$  K.<sup>(c)</sup> From [36];  $T = 300$  K.<sup>(d)</sup> From [12];  $T = 77$  K.<sup>(e)</sup> See figure 5.<sup>(f)</sup> From table 1 of [8];  $T = 300$  K.<sup>(g)</sup> From [18].

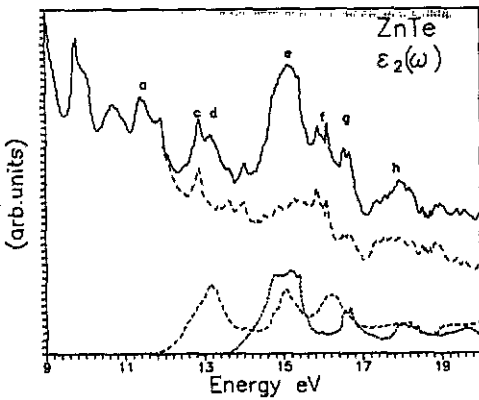
We attempted to compare our theoretical results with those of the experimental study of reflectivity of ZnTe, CdTe and HgTe presented in [8]. The experimental reflectivity spectra of ZnTe and CdTe are reproduced from [8] and presented in figure 7. The direct comparison is difficult on account of the well-known deficiencies of LDA. Further, the basis function set is limited to  $ns$ ,  $np$  and  $(n-1)d$  for cation and  $5s$ ,  $5p$ ,  $5d$  for anion and also calculations do not include spin-orbit coupling so that the number of interband contributions is reduced. Our results are obtained within the framework of the one-electron approximation, so that observed deviations from the experimental amplitudes and peak positions might be attributed to many-body effects. We will show, however, that despite this our calculations allow for a consistent interpretation of the optical spectra.

Curves depicted in figures 4, 5, 6 were calculated without the inclusion of the effects of the finite relaxation time [18]. In the interpretation of the optical spectrum above 9 eV we concentrate on the structures associated with the excitation of the metal d levels. The theoretical, adjusted spectrum of  $\epsilon_2(\omega)$  is characterized by the structures labelled a, c, d, e, f, g and h in figures 4, 5 and 6 and in tables 4, 5 and 6. The peaks d and e can be associated with transitions from the d levels to the first and the second conduction bands respectively. The origin of the other peaks is difficult to identify unequivocally on account of a very significant contribution from the transitions originating in the upper



**Table 6.** Experimental and theoretical values (in eV) of energy gaps in HgTe compared to the LDA values calculated in this work.

| Peak   | Experimental        | Other calculations   | Present calculations |          |
|--------|---------------------|----------------------|----------------------|----------|
|        |                     |                      | unadjusted           | adjusted |
| $E_0$  | -0.3 <sup>(c)</sup> | -0.28 <sup>(a)</sup> | -0.8                 | -0.3     |
| $E_1$  | 2.22 <sup>(c)</sup> | 2.22 <sup>(a)</sup>  | 1.70                 | 2.22     |
| $E_2$  | 4.9 <sup>(b)</sup>  | 4.55 <sup>(a)</sup>  | 4.26                 | 5.0      |
|        | 5.10 <sup>(c)</sup> | —                    | 4.70                 | —        |
| $E'_1$ | 6.57 <sup>(b)</sup> | —                    | 5.96                 | 6.68     |
| a      | —                   | —                    | 11.24                | 11.76    |
| c      | 10.2 <sup>(b)</sup> | —                    | 9.56                 | 10.07    |
| d      | 10.8 <sup>(b)</sup> | —                    | 9.56                 | 10.80    |
| e      | 12.8 <sup>(b)</sup> | —                    | 11.62                | 12.84    |
| f      | 13.5 <sup>(b)</sup> | —                    | 12.66                | 13.86    |
| g      | 16.2 <sup>(b)</sup> | —                    | 15.72                | 16.24    |
| h      | 18.3 <sup>(b)</sup> | —                    | 17.76                | 18.30    |

<sup>(a)</sup> See [1].<sup>(b)</sup> From table 1 of [8];  $T = 300$  K.<sup>(c)</sup> See [22];  $T = 15$  K.**Figure 4.** Absorption spectrum  $\epsilon_2^b(\omega)$  in the region of the cation d excitations (adjusted case) for ZnTe.

part of the valence band to the higher conduction bands. Nevertheless, the agreement with the experimental results and the discussion presented in paper [8] is quite satisfactory. The largest discrepancy is found in the interpretation of the a peak in the  $\epsilon_2(\omega)$  spectra. The suggestion that the a peak of ZnTe, CdTe and HgTe is a core exciton [8, 25] seems to be in error. We interpret this sharp peak at 11.65 eV (ZnTe), 12.10 eV (CdTe), and 11.76 eV (HgTe) as transitions from the 8th and 9th bands to the 14th band. We have also determined the regions in  $k$  space giving the major contributions to the intensity of the peaks in  $\epsilon_2(\omega)$ . For all three semiconductors studied here we find that essentially the same  $k$  points give rise to the major part of the intensity of the peaks. The calculated static dielectric constant  $\epsilon(0)$  is found to be 5.0 for ZnTe, 5.4 for CdTe and 19.3 for HgTe, whereas the experimental values are 7.3, 7.2 and 21.0 [26]. This difference is mainly due to the local field not taken into account in our calculation [18].

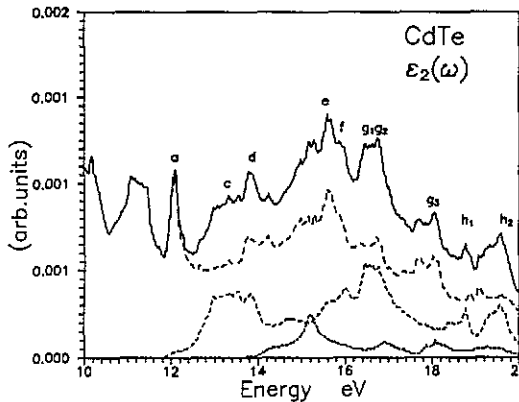


Figure 5. Absorption spectrum  $\epsilon_2^2(\omega)$  in the region of the cation d excitations (adjusted case) for CdTe.

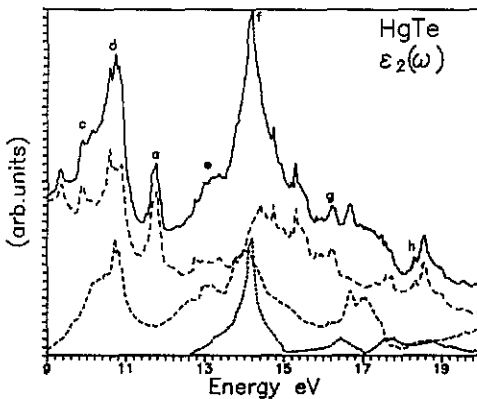


Figure 6. Absorption spectrum  $\epsilon_2^2(\omega)$  in the region of the cation d excitations (adjusted case) for HgTe.

#### 4. Conclusion and summary

On the basis of the preceding discussion, the results obtained in this work can be summarized as follows.

We calculated the real and imaginary parts of the dielectric functions as well as the reflectivity spectra up to 20 eV for the semiconducting compounds ZnTe, CdTe and HgTe using the self-consistent band structures obtained by the LMTO method.

As expected, the LD approximation gives the ground state properties accurately but the resulting band structures are different in detail from those found experimentally. The simplest calculation, one panel and scalar relativistic corrections, provides results for  $\epsilon_1(\omega)$ ,  $\epsilon_2(\omega)$  and  $R(\omega)$  spectra which are not easy to interpret.

To allow a direct comparison between theory and experiment, a very simple procedure of energy band shifting is applied.

In general, our calculations allow for a consistent assignment of structures in the experimental reflectivity spectra for the materials examined and for understanding the physical mechanism of the transitions observed in the  $R(\omega)$  spectra.

We show that interpretation of the UV part of the spectra proposed by Cardona *et al* [12] and Kisiel *et al* [8] is not entirely correct. In particular, the role of the transitions

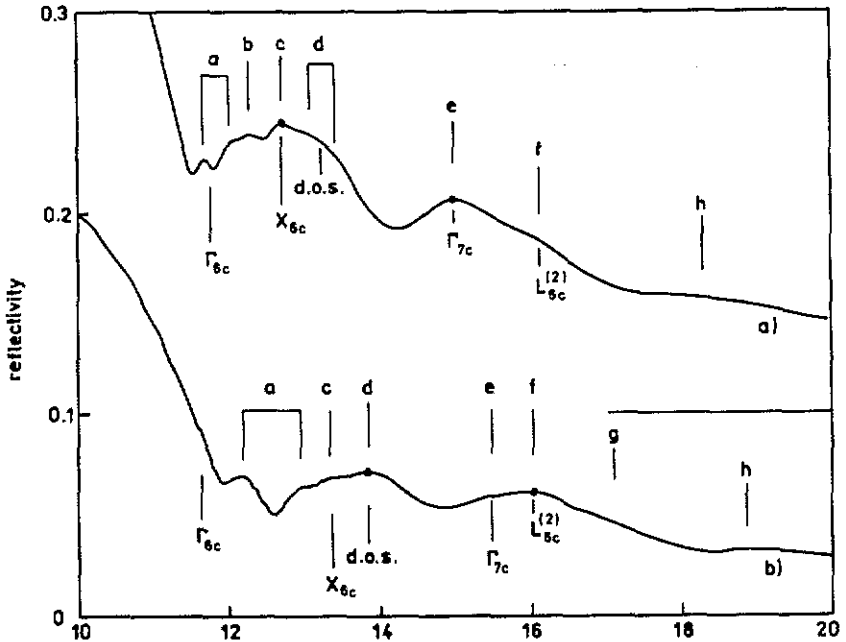


Figure 7. Reflectivity spectra of a) ZnTe (shifted upwards by 0.1) and b) CdTe measured at room temperature in the region of cation d excitations. The assignments of the observed structures are also indicated (see [8]).

from the upper valence bands is not properly recognized in these papers. Contrary to common belief, apart from the strong contribution from the metal d states transitions, we find in this energy range a very significant contribution from transitions originating in the upper part of the valence band with final states in the higher conduction bands.

We also suggest that structures in the reflectivity spectra assigned to core excitons can be described within the framework of a band-to-band transition formalism.

In order to obtain an improved band structure for II-VI compounds, particularly narrow-gap semiconductors such as HgTe, it is necessary to include all relativistic effects i.e. Darwin and mass-velocity corrections and spin-orbit interactions, as has been shown by Kisiel and Lee [4]. So the more detailed calculation with s-o interaction included self-consistently and the basis function set extended to cation  $nd$  functions should be carried out to produce  $\epsilon_2(\omega)$  and  $R(\omega)$  spectra which would give a better interpretation of the data.

### Acknowledgments

We are grateful to Professor A Kisiel for suggesting this work and for many stimulating discussions. We should like to thank Professor P M Lee of the University of Lancaster for his valuable comments.

### References

- [1] Czyżyk M T and Podgórný M 1980 *Phys. Status Solidi* b 98 507

- [2] Chelikowsky J R and Cohen M L 1976 *Phys. Rev. B* **14** 556
- [3] Walter J P, Cohen M L, Petroff Y and Balkanski M 1970 *Phys. Rev. B* **1** 2661
- [4] Kisiel A and Lee P M 1972 *J. Phys. F: Met. Phys.* **2** 395
- [5] Hass K C, Ehrenreich H and Velicky B 1983 *Phys. Rev. B* **27** 1088
- [6] Cade N A and Lee P M 1985 *Solid State Commun.* **56** 637
- [7] Christensen N E and Christensen O B 1986 *Phys. Rev. B* **33** 4739
- [8] Kisiel A, Zimnal-Starnawska M, Antonangeli F, Piacentini M and Zema N 1986 *Nuovo Cimento D* **8** 436
- [9] Cardona M, Shaklee K L and Pollak F H 1967 *Phys. Rev.* **154** 696
- [10] Taniguchi M, Ley L, Johnson R L, Ghijsen J and Cardona M 1986 *Phys. Rev. B* **33** 1206
- [11] Vesely C J and Langer D W 1971 *Phys. Rev. B* **4** 451
- [12] Cardona M and Greenaway D L 1963 *Phys. Rev.* **131** 98
- [13] Andersen O K 1975 *Phys. Rev. B* **12** 3060
- [14] Markowski R and Podgórnny M 1991 *J. Phys.: Condens. Matter* **3** 9041
- [15] Vosko S H, Wilk L and Nusair M 1980 *Can. J. Phys.* **58** 1200
- [16] Jarlborg T and Freeman A J 1976 *Phys. Lett.* **74A** 399
- [17] Gloetzel D, Segall B and Andersen O K 1980 *Solid State Commun.* **36** 403
- [18] Alouani M, Brey L and Christensen N E 1988 *Phys. Rev. B* **37** 1167
- [19] Koenig C and Khan M A 1983 *Phys. Rev. B* **27** 6129
- [20] Alouani M, Koch J M and Khan M A 1986, *J. Phys. F: Met. Phys.* **16** 473
- [21] Petroff Y, Balkanski M, Walter J P and Cohen M L 1968 *Solid State Commun.* **7** 459
- [22] Chadi D J, Walter J P, Cohen M L, Petroff Y and Balkanski M 1972 *Phys. Rev. B* **5** 3058
- [23] Wei S H and Zunger A 1988 *Phys. Rev. B* **37** 8958
- [24] Sherchik N J, Tejada J, Cardona M and Langer D W 1973 *Phys. Status Solidi b* **59** 87
- [25] Aspens D E, Olson C G and Lynch D W 1975 *Phys. Rev. B* **12** 2527
- [26] Harrison W A 1980 *Electronic Structure and the Properties of Solids* (San Francisco: Freeman)
- [27] Kurganski S I, Farberovich O W and Domashevskaia E P 1980 *Phys. Techn. Semicond.* **14** 1315.
- [28] Rodzik A and Kisiel A 1983 *J. Phys. C: Solid State Phys.* **16** 203
- [29] Ley L, Pollak R A, McFeely F R, Kowalczyk S P and Shirley D A 1974 *Phys. Rev. B* **9** 600
- [30] Au-Ban Shen and Sher A 1982 *J. Vac. Sci. Technol.* **21** 138
- [31] Kisiel A, Podgórnny M, Rodzik A and Giriat W 1975 *Phys. Status Solidi b* **70** 767
- [32] Matatagai E, Thompson A G and Cardona M 1968 *Phys. Rev.* **176** 950
- [33] Moritani A, Taniguchi K, Hamaguchi C M and Nakai J 1973 *J. Phys. Soc. Japan* **34** 79
- [34] Guizzetti G, Nosenzo L, Reguzzoni E and Samoggia G 1974 *Phys. Rev. B* **9** 640
- [35] Thomas D G 1961 *J. Appl. Phys.* **32** 939
- [36] Lautenschlager P, Logothetidis S, Vina L and Cardona M 1985 *Phys. Rev. B* **32** 3811
- [37] Mei J R and Lemos V 1984 *Solid State Commun.* **52** 785